Germline V-genes sculpt the binding site of a family of antibodies neutralizing human cytomegalovirus

Christy A Thomson[1], Steve Bryson[2], Gary R McLean[1,5], A Louise Creagh[3], Emil F Pai[4] and John W Schrader[1,*]

[1]The Biomedical Research Centre, University of British Columbia, Vancouver, British Columbia, Canada, [2]Department of Biochemistry, University of Toronto, and Division of Cancer Genomics & Proteomics, Ontario Cancer Institute, Toronto, Ontario, Canada, [3]Michael Smith Laboratories and the Department of Chemical and Biological Engineering, University of British Columbia, Vancouver, British Columbia, Canada and [4]Departments of Biochemistry, Medical Biophysics and Molecular Genetics, University of Toronto, and Division of Cancer Genomics & Proteomics, Ontario Cancer Institute, Toronto, Ontario, Canada

Immunoglobulin genes are generated somatically through specialized mechanisms resulting in a vast repertoire of antigen-binding sites. Despite the stochastic nature of these processes, the V-genes that encode most of the antigen-combining site are under positive evolutionary selection, raising the possibility that V-genes have been selected to encode key structural features of binding sites of protective antibodies against certain pathogens. Human, neutralizing antibodies to human cytomegalovirus that bind the AD-2S1 epitope on its gB envelope protein repeatedly use a pair of well-conserved, germline V-genes *IGHV3-30* and *IGKV3-11*. Here, we present crystallographic, kinetic and thermodynamic analyses of the binding site of such an antibody and that of its primary immunoglobulin ancestor. These show that these germline V-genes encode key side chain contacts with the viral antigen and thereby dictate key structural features of the hypermutated, high-affinity neutralizing antibody. V-genes may thus encode an innate, protective immunological memory that targets vulnerable, invariant sites on multiple pathogens.

*Corresponding author. The Biomedical Research Centre, University of British Columbia, 2222 Health Sciences Mall, Vancouver, British Columbia, Canada V6T 1Z3. Tel.: +1 604 822 7822; Fax: +1 604 822 7815; E-mail: john@brc.ubc.ca
[5]Present address: Department of Respiratory Medicine, Imperial College, London, UK

Introduction

Human cytomegalovirus (HCMV) is a member of the family Herpesviridae that also includes herpes simplex virus and Epstein–Barr virus. HCMV co-evolved with humans (McGeoch *et al*, 2000) and although 50–90% of humans are chronically infected with HCMV, it rarely causes harm because it is kept in check by the immune system. However, HCMV can cause serious and sometimes fatal disease (retinitis, pneumonitis and hepatitis) in adults who are immunocompromised by AIDS or immunosuppressive drugs. Moreover, about 1% of susceptible women acquire a primary infection during pregnancy, with 40% of these women transmitting CMV to their fetuses, often causing death or severe neurological defects (Boppana *et al*, 1992; Duff, 2005). No protective vaccine is currently available. Recent evidence indicates that the administration of pooled human immunoglobulins (that contain antibodies that neutralize HCMV) reduces the incidence of congenital abnormalities in neonates born to mothers who suffer from primary HCMV infections during pregnancy (Nigro *et al*, 2005). HCMV can be neutralized by antibodies that target a short, linear epitope on the gB envelope protein of HCMV termed AD-2S1 (amino-acid sequence: ETIYNTTLKY), which is thought to serve an important function in viral infectivity (Meyer *et al*, 1990; Ohizumi *et al*, 1992). Intriguingly, although the three different families of human antibodies specific for AD-2S1, for which sequences are available, were independently derived from two unrelated individuals, all were derived from the same pair of V-genes (*IGHV3-30* and *IGKV3-11*) (Ohlin *et al*, 1993; McLean *et al*, 2005). Similarly, a fourth family of heavy chain sequences of anti-AD-2S1 antibodies were analysed from a third individual and found to use the same VH gene (*IGHV3-30*) (McLean *et al*, 2005). On the basis of the frequency of use of these V-genes in human B lymphoid cells (0.048 and 0.12, respectively) (Lefranc *et al*, 2005), the probability that this pair of V-genes was used by chance in these three independently generated sets of anti-AD-2S1 antibodies is vanishingly small (0.0000002). Rather the consecutive use of this pair of V-genes suggests that this pair of V-genes make critical contributions to encoding a preferred binding site for AD-2S1. This is consistent with other evidence for the preferential use of V-genes in antibodies against haptens (Makela and Kaartinen, 1988). However, the fact that the AD-2S1 epitope is the target of antibodies that block infectivity with a common pathogen raises the possibility that these V-genes have undergone evolutionary selection to facilitate the generation of a binding site for this epitope.

Immunoglobulin genes represent the largest and most diverse class of genes in any organism. Throughout life, random pairs of novel heavy and light chain immunoglobulin genes are assembled in each newly generated B lymphocyte. The immunoglobulin H- and L-chain genes each encode three
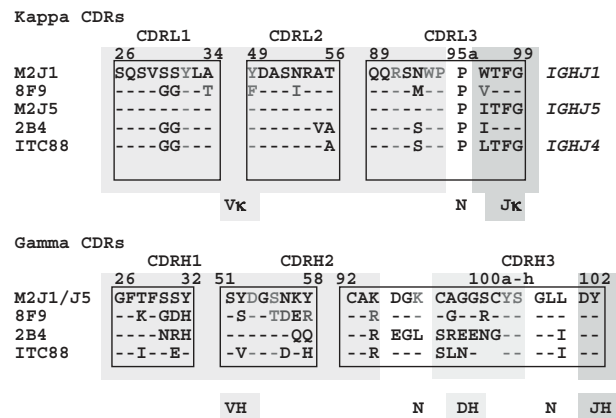
of the six variable 'complementarity determining regions' (CDRs) that make up the antigen-combining site of immunoglobulins. The amino-acid sequences of these CDRs are extremely variable, accounting for the structural diversity of the antigen-combining sites of immunoglobulins and their enormous repertoire of binding specificities. Further combinatorial diversity is generated by variation in the precise sites at which recombination occurs, as well as by the addition of untemplated bases at sites of recombination by the enzyme terminal deoxynucleotidyl transferase (TdT) (Desiderio *et al*, 1984; Thai *et al*, 2002). The V-genes encode the N-terminal portion of their respective H- or L-chains, including CDR1, CDR2 and part of CDR3. The remaining parts of the CDR3s are encoded by somatically generated DNA sequences formed by the stochastic recombination of V- and J-genes (L-chains) or V-, D- and J-genes (H-chains). Encounter with their cognate antigen stimulates B lymphocytes to undergo a further unique process, termed 'affinity maturation'. This results in somatic mutations in the immunoglobulin genes, and competitively selects for B lymphocytes that are making mutated immunoglobulins with higher affinity for the specific antigen.

Despite the stochastic nature of the processes that generate the genes encoding a high-affinity antibody, certain V-genes are used more frequently than others in antibodies to certain pathogens (Insel *et al*, 1992; Muller *et al*, 1993; Zhou *et al*, 2002). This has given rise to speculation that V-genes have been selected to encode parts of the binding sites for components of common pathogens. However, a non-mutually exclusive alternative is that V-genes have been selected to encode conformational flexibility in the combining sites of primary immunoglobulins, enabling the latter to bind multiple antigens (Wedemayer *et al*, 1997; Manivel *et al*, 2000, 2002; James *et al*, 2003; Notkins, 2004). Certainly, human V-genes are evolving fast and are under positive selective pressure (Tanaka and Nei, 1989; Insel *et al*, 1992; Muller *et al*, 1993; Zhou *et al*, 2002). Here, we describe the structure of a protective antibody against a common pathogen that co-evolved with humans, which shows for the first time that a pair of well-conserved, frequently used, human V-genes encode the residues that make key contacts with a critical site of a pathogenic virus. Interestingly, in keeping with other data on affinity maturation, the high-affinity, somatically mutated antibody did not exhibit any new direct contacts between the antigen and the side chains of the amino acids of the CDRs. Instead, the somatic mutations that were selected for stabilized and enhanced the germline-encoded interactions with the antigen. Thus, due to the physicochemistry of affinity maturation, these well-conserved V-genes dictate the key contacts of the high-affinity neutralizing antibody with its target.

Results

Kinetics

The hypermutated, high-affinity, neutralizing human monoclonal antibody 8F9, similar to other known human antibodies against the AD-2S1 epitope of gB for which sequence information is known, uses two highly conserved V-genes (*IGHV3-30* and *IGKV3-11*). For kinetic, thermodynamic and structural characterization of the 8F9–AD-2S1 interaction, the Fab fragment of 8F9 was expressed in *Escherichia coli* and

```
Kappa CDRs
           CDRL1         CDRL2         CDRL3
         26      34    49      56    89    95a   99
M2J1     SQSVSSYLA     YDASNRAT      QQRSNWP P WTFG   IGHJ1
8F9      ----GG--T     F---I----     ------M-- P V---
M2J5     ---------     ---------     -------- P ITFG   IGHJ5
2B4      ----GG---     ------VA      ----S-- P I---
ITC88    ----GG---     -------A      ----S-- P LTFG   IGHJ4

              Vκ                        N    Jκ


Gamma CDRs
           CDRH1         CDRH2                 CDRH3
         26    32      51      58  92        100a-h      102
M2J1/J5  GFTFSSY       SYDGSNKY    CAK DGK CAGGSCYS GLL DY
8F9      --K-GDH       -S--TDER    --R --- -G--R--- --- --
2B4      ----NRH       ------QQ    --R EGL SREENG-- --I --
ITC88    --I--E-       -V---D-H    --R --- SLN-  -- --I --

             VH              N     DH    N    JH
```

Figure 1 Alignments of the CDRs of the primary immunoglobulins (M2J1 & M2J5) and hypermutated antibodies (8F9, 2B4 and ITC88). Residues highlighted in red are those whose side chains directly contact AD-2S1. Residues highlighted in blue are those somatic mutations that occurred in 8F9 that stabilize the binding site. A full-colour version of this figure is available at *The EMBO Journal* online.

purified. To examine the effects of somatic mutation and affinity maturation on the structure and function of the AD-2S1-binding site, and to assess the contribution of the germline V-genes to the generation of a high-affinity neutralizing antibody, we analysed in parallel the Fab fragment of the primary, unmutated ancestor of 8F9, M2J1 (McLean *et al*, 2005). We also analysed the Fab fragment of a closely related primary immunoglobulin, M2J5, which differed from M2J1 only in that its L-chain gene resulted from recombination of *IGKV3-11* with *IGKJ5* rather than *IGKJ1* (Figure 1). The L-chain gene used in M2J5 was used in the ancestral primary immunoglobulin of 2B4, another neutralizing antibody against AD-2S1 that also used *IGHV3-30* and *IGKV3-11* and arose independently in the same donor as 8F9 (McLean *et al*, 2005).

The Fab fragments of 8F9, M2J1 and M2J5 had the same relative abilities to bind AD-2S1 as the corresponding immunoglobulin molecules (Supplementary Figure 1). As measured by isothermal titration calorimetry (ITC), the affinity of 8F9 Fab for the AD-2S1 peptide was in the nanomolar range (94 nM), whereas binding of M2J5 Fab to AD-2S1 was about 200-fold weaker (20 μM) (Table I). The affinity of the ancestral M2J1 Fab for AD-2S1 approached the practical limits of measurement by this technique (10^{-3} M) and from ELISA data was probably 10-fold lower than that of M2J5. The surface plasmon resonance (SPR) analysis of the binding of 8F9 Fab to the AD-2S1 peptide gave a similar K_D value (120 nM) to that determined by ITC, and indicated that there was a fast on-rate (3.5 e^5 M^{-1} s^{-1}) but also a fast off-rate (0.04 s^{-1}) (Table I). The low affinity of M2J1 and M2J5 Fabs did not allow accurate determinations of the on-rates and off-rates by SPR. It is important to note that, although the affinities of M2J1 and M2J5 are low, they are within the threshold of affinity of the immunoglobulin required for effective antigen-induced activation of B lymphocytes, which is as low as 10^{-4} M (Lang *et al*, 1996). This reflects the fact that, *in vivo*, both the antigen and the immunoglobulin receptor occur in multivalent arrays and avidity effects dominate (Batista and Neuberger, 1998; Qi *et al*, 2006).

Table I Kinetic and thermodynamic characterization of the binding of 8F9 Fab and M2J5 Fab to AD-2S1

	Biacore analysis			ITC analysis					
	k_a (1 M^{-1} s^{-1})	k_d (1 s^{-1})	K_D (nM)	K_D (nM)	$\Delta G°$ (kcal mol^{-1})	$\Delta H°$ (kcal mol^{-1})	$\Delta S°$ (cal mol^{-1} K^{-1})	n	T (K)
8F9	2.5×10^5	8.5×10^{-3}	34	—	—	—	—	—	285
	—	—	—	43	−9.2	−11.4	−6.2	1.2	287
	3.5×10^5	0.04	120	94	−9.3	−14.3	−16	1.2	297
	—	—	—	240	−9.3	−16	−21.9	1.2	307
M2J5	—	—	—	4600	−7	−6.7	0.8	0.93	287
	—	—	—	19 000	−6.4	−11.2	−16.1	0.95	297
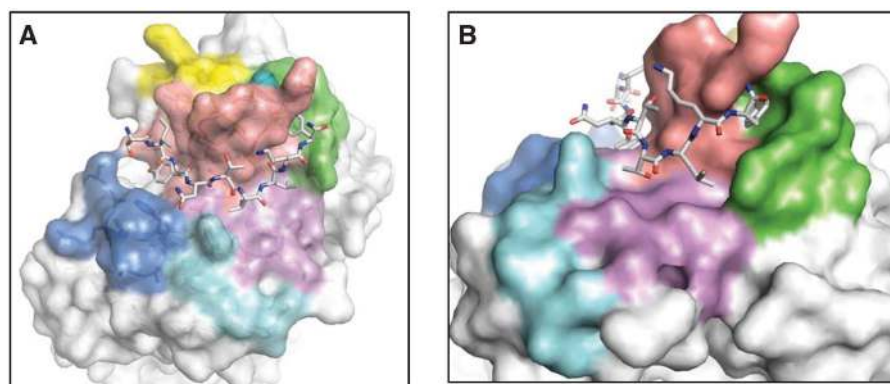
Figure 2 (**A**, **B**) Structure of 8F9 Fab complexed with the AD-2S1 peptide. The AD-2S1 peptide (shown in CPK coloring) is in an extended conformation as it wraps around CDRH3 (pale red). The P10-Tyr found in a hydrophobic pocket formed by CDRH2 and the base of CDRH3. The L-chain interacts with peptide side chains through nonpolar van der Waals interactions, whereas the H-chain contributes backbone hydrogen bonds to the peptide backbone atoms. CDRL1 is light blue; CDRL2 is dark blue; CDRL3 is purple; CDRH1 (which does not contact the peptide) is yellow; CDRH2 is green and CDRH3 is pale red. A water molecule bridging the CDRH2 and CDRH3 loops is shown in aqua.

The complex of the 8F9 Fab and the AD-2S1 peptide

The crystal structure of the complex of the 8F9 Fab and the AD-2S1 peptide ([69]ETIYNTTLKY[78]), refined at 2.3 Å resolution, is shown in Figure 2 and Supplementary Figure 2. The AD-2S1 peptide backbone forms an arc that wraps around CDRH3 in an extended conformation, making a network of hydrogen bonds with CDRH3 backbone atoms. CDRH2 and CDRH3 form a binding pocket for the side chain of the C-terminal residue of the peptide, P10-Tyr. The N-terminal residue of the peptide, P1-Glu, was not modelled due to the lack of electron density. CDRH1 does not interact with the peptide. All three CDR loops of the L-chain contact peptide side chains (P4-Tyr, P7-Thr, P8-Leu and P10-Tyr). Strikingly, these were the four residues in AD-2S1 that were previously identified as being critical for the recognition of AD-2S1 by ITC88, another high-affinity, neutralizing monoclonal antibody against HCMV that was generated from another human and that also used the *IGHV3-30* and *IGKV3-11* V-genes (Figure 1) (Ohlin *et al*, 1993). Indeed, all other side chains of the peptide point away from the 8F9 paratope. Alanine substitutions of any of these four residues in the AD-2S1 peptide abrogated binding of ITC88, indicating that each of these side chain contacts contributed to binding (Ohlin *et al*, 1993). Additional evidence for the importance of binding of contacts with the P10-Tyr comes from observations on the reactivity of 8F9 and M2J1 with the homologue of the AD-2S1 peptide in chimpanzee CMV (CCMV), (EYIFNTTLRP). The P4-Phe should make the same interactions with 8F9 as the P4-Tyr in human AD-2S1 as the hydroxyl group of P4-Tyr

does not interact with 8F9. In keeping with the prediction that the substitution of P10-Tyr with Pro should decrease binding, 8F9 bound only poorly to the homologue of CCMV peptide, whereas M2J1 failed to bind at all (McLean *et al*, 2006).

CDR1 of the L-chain contributes two key residues in the binding of AD2-S1. The germline-encoded Tyr-32(L) is the only residue of this loop to contact the peptide directly and provides a nonpolar surface for the γ-carbon of P7-Thr of the peptide (Figure 3A). It also stacks against a methylene group of the germline-encoded CDR-L3 residue Arg91(L). The other residue, Thr-34(L), mutated from the germline Ala sits below residue Arg-91(L), providing it support with its hydroxyl moiety contacting a water molecule that contacts the guanidinium group of Arg-91(L). In addition, its γ-carbon forms part of a series of van der Waals interactions involving the hydrophobic residues Tyr-36(L), Leu-46(L) and Leu-111(H), which form a hydrophobic surface for the P4-Tyr residue of the peptide.

CDRL2 also provides a key contact with the peptide. The phenol ring of P4-Tyr stacks perpendicularly with Phe-49(L) (Figure 3B). Although, in 8F9, Phe-49(L) has been mutated from the germline-encoded Tyr-49(L), inspection of the structure of M2J1 shows that the germline-encoded Tyr-49 would provide the same stacking arrangement with the P4-Tyr side chain. In support of this conclusion, the germline-encoded Tyr-49(L) was not mutated in any of eight other hypermutated anti-AD-2S1 antibodies analysed to date, including ITC88 and the 2B4 family of antibodies (Figure 1).
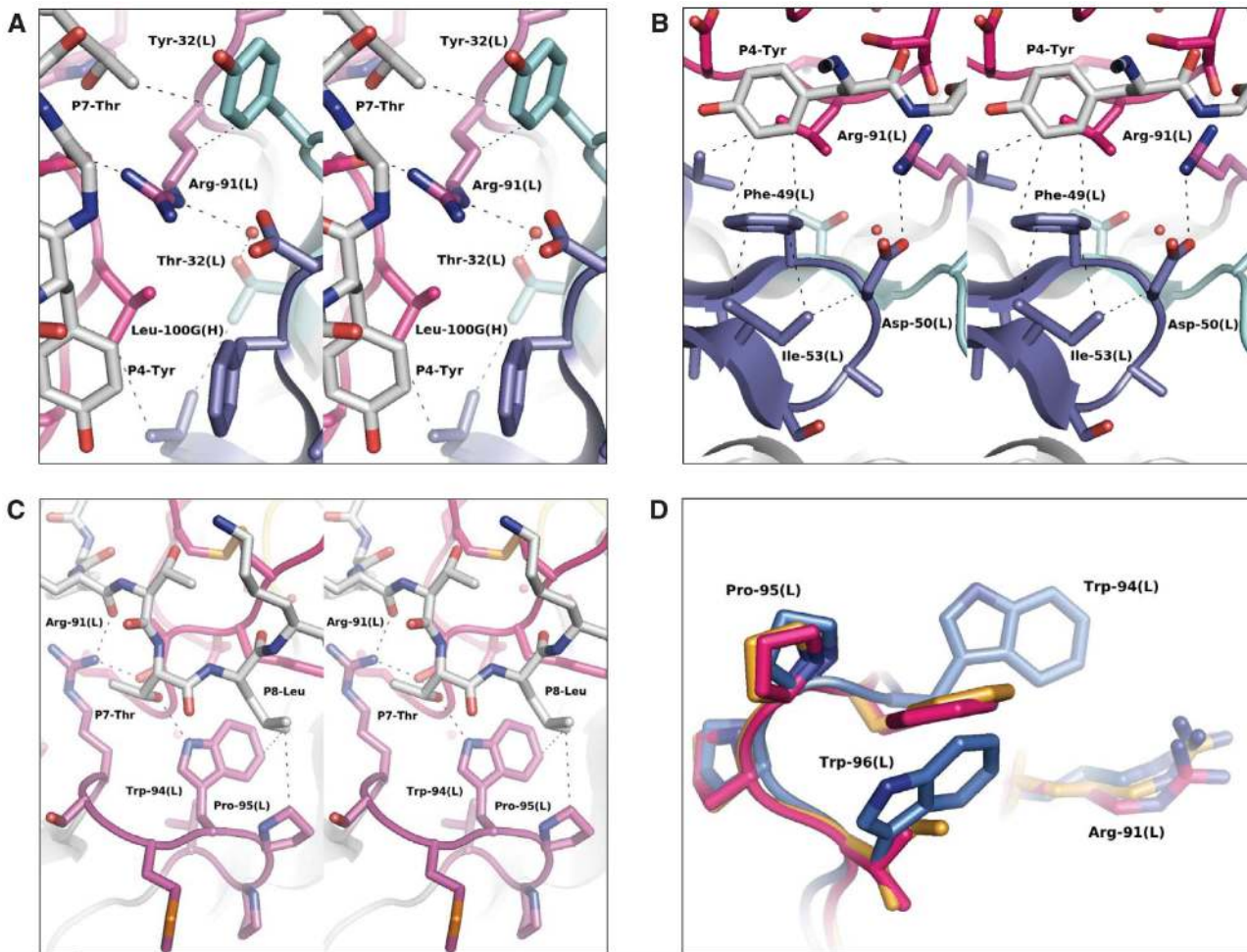
Figure 3 Light chain interactions. A, B and C are in cross-eyed stereo. (**A**) CDRL1 residue interactions (light blue). Tyr-32(L) stacks against P7-Leu and Arg-91(L). A water molecule (red sphere) bridges Thr-32(L) and Arg-91(L). The hydroxyl group of Thr-32(L) makes hydrophobic contacts. (**B**) CDRL2 residue interactions (dark blue). P4-Tyr stacks on Phe-49(L), which is supported by Ile-53(L). Ile-53(L) also supports Asp-52(L) that makes a hydrogen bond with Arg-91(L). (**C**) CDRL3 residue interactions (purple). Trp-94(L) and Pro-95(L) form a hydrophobic pocket to accommodate P8-Leu. Arg-94(L) also forms a hydrogen bond with the side chain of P7-Thr. (**D**) Conformation of Trp-94(L) differs in M2J1. The conformation of Trp-94(H) is displaced in M2J1 where the sequence contains a tryptophan at position 96(H) (blue). When residue 96(H) is a small hydrophobic residue such as Val96(H) in 8f9 (red) or Ile-96(H) in M2J5.

The interaction of Phe-49(L) with P4-Tyr is supported by the somatically mutated nonpolar residue Ile-53(L). The δ-carbon of Ile-53(L) also supports the germline-encoded Asp-50(L) through contact with its β-carbon. Germline-encoded Asp-50(L) in turn forms a salt bridge with the critical germline residue, Arg-91(L), stabilizing the tight turn of CDRL2.

CDRL3 forms a hydrophobic pocket for P8-Leu that is sculpted by two germline V-gene-encoded residues, Trp-94(L) and Pro-95(L) (Figure 3C). Trp-94(L) makes another contact with a side chain of AD2-S1, as the ε-carbon of its indole ring forms a hydrogen bond with the hydroxyl group of P7-Thr. We previously showed that in M2J1, mutation of the germline Trp-96(L) to the Val found in 8F9 greatly increased binding to AD-2S1 (McLean *et al*, 2005). Comparison of the crystal structures of the 8F9 and M2J1 and M2J5 Fab fragments reveals why. In M2J1, the large bulky Trp-96(L) displaces Trp-94(L) upwards, disrupting its interaction with P7-Thr and P8-Leu (Figure 3D). In M2J5, which is identical to M2J1 except for the use of a germline *IGKJ5* gene rather than the *IGKJ1* gene, Trp-96(L) is replaced

by the small hydrophobic residue Ile-96(L). Inspection of the crystal structure of the M2J5 Fab (Figure 3D) shows that this germline V-gene-encoded Ile, similar to the Val in 8F9, also permits a favourable orientation of Trp-94(L) for interaction with P8-Leu, explaining why M2J5 has a much higher affinity for AD-2S1 than M2J1. In antibodies of the other two families of hypermutated anti-AD-2S1 antibodies that use these V-genes, for example, ITC88 or 2B4 (Figure 1), the residues at position 96(L) are also small hydrophobic residues encoded by the germline J genes (Ile, encoded by *IGKJ5* in 2B4, or Leu, encoded by *IGKJ4*, in ITC88). The germline-encoded Arg-91(L) is also very important for the binding site. In addition to the interactions mentioned, it forms a H-bond with the backbone carbonyl of P5-Asn at 2.8 Å and with the backbone carbonyl of Ser-109(H) at the base of the CDRH3 loop (Figure 3C).

Although CDRH1 does not contact the AD2-S1 peptide, it does make a network of specific interactions that are important for supporting the conformation of the CDRH3 loop (Figure 4A). The nitrogen atom of the His-32(H) imidazole ring makes a H-bond (3.1 Å) with the backbone
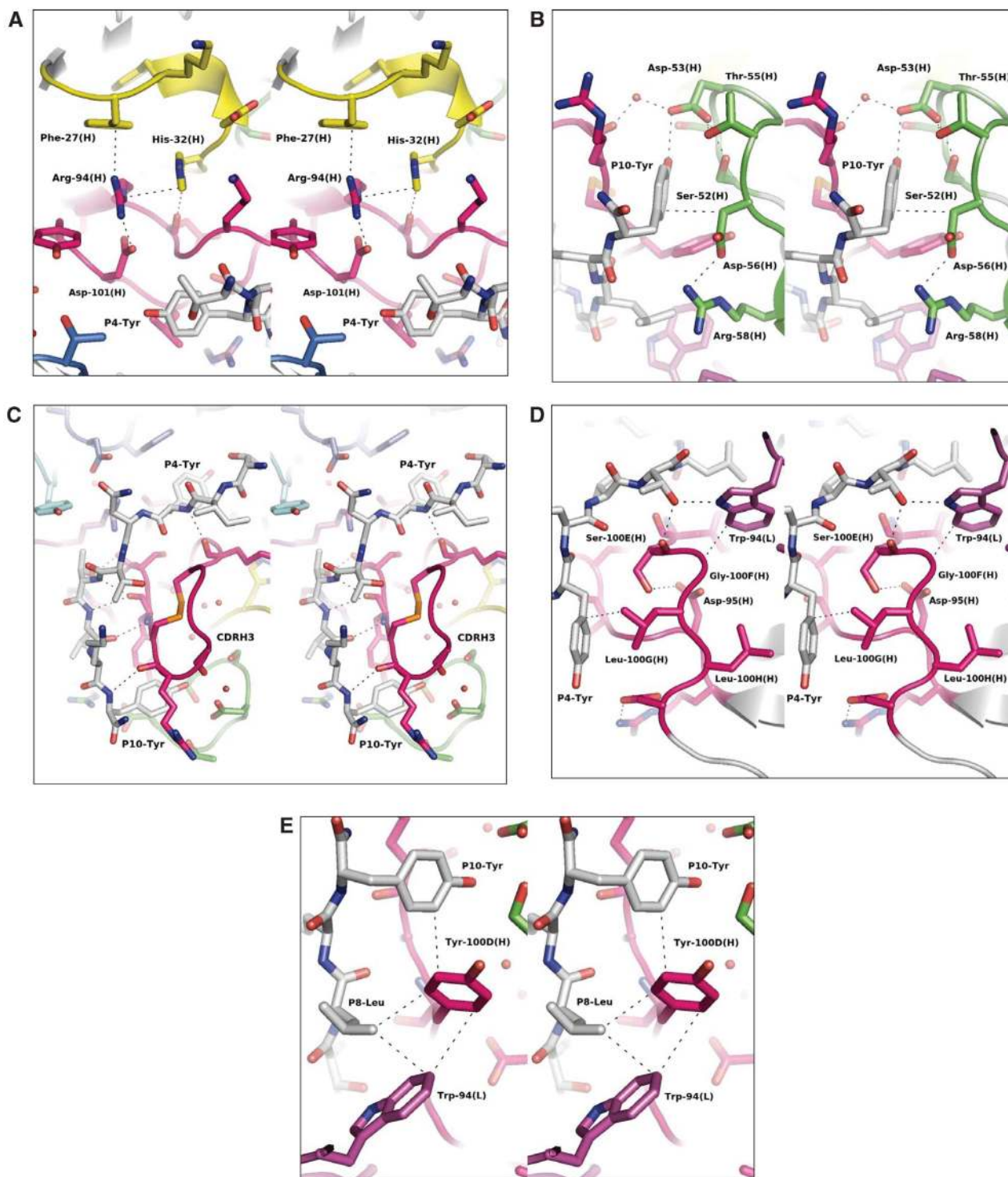
Figure 4 Heavy chain interactions (cross-eyed stereo). (**A**) CDRH1 residue interactions (yellow). His-32(H) and Phe-27(H) support CDRH3 base residue Arg-94(H) through stacking interactions. Arg-94(H) in turn contacts base residue Asp-101(H). (**B**) CDRH2 residue interactions (green). Asp-53(H) forms a hydrogen bond with the hydroxyl group of P10-Tyr at the base of the pocket. Asp-53(H) is positioned by Ser-52(H) and Thr-55(H) and a water molecule that bridges the CDRH2 and CDRH3 loops. The opening of the pocket is stabilized by the salt bridge created between Asp-56(H) and Arg-58(H). (**C**) CDRH3 residue interactions (red). The extended conformation of the peptide wraps around the CDRH3 loop interacting through a series of backbone–backbone hydrogen bonds (indicated). (**D**) SGLL motif interactions (red). Ser-100E(H) forms a hydrogen bond with Asp-95(H) stabilizing the base of the CDRH3 loop. The α-carbon of Gly-100F(H) contacts the indole ring of Trp-94(L). Leu-100G(H) forms the base of the hydrophobic pocket that bind P4-Tyr. Leu-100H(H) is part of the hydrophobic pocket supporting Trp-94(L). (**E**) Role of Tyr-100D(H). Tyr-100D(H) creates the base of the P10-Tyr-binding pocket. It also stacks against Arg-94(L) as part of the P8-Leu hydrophobic binding pocket.

carbonyl of Asp-99(H) and the plane of the ring is parallel with the plane of the guanidine moiety (3.9 Å) of Arg-94(H) at the base of the CDRH3 loop. Arg-94(H) also forms a π-cation

stacking arrangement with CDRH1 residue Phe-27(H) and a tight hydrogen bond to Asp-113(H) at the base of the CDRH3 loop.

CDRH2, on the other hand, forms a network of hydrogen bonds to the P10-Tyr hydroxyl group (Figure 4B). In particular, the P10-Tyr hydroxyl directly contacts the germline V-gene-encoded Asp-53(H) that in turn is positioned by the side chain hydroxyl of Thr-55(H) and Ser-52(H). In the unmutated primary immunoglobulin, M2J1, Thr-55(H) residue is a Ser, which would most likely make the same contact with Asp-53(H). Consistent with this conclusion, Ser-55(H) was not mutated to a Thr-55(H) in any of the other eight neutralizing, hypermutated anti-AD-2S1 antibodies, for example, 2B4 or ITC88 (Figure 1). The mutated Asp-56(H) is positioned at the entrance of the P10-Tyr pocket and is held in the 'open' position by the guanidinium group of Arg-58(H). This conformation creates a stacking arrangement between the Asp-56(H) β-carbon and the P10-Tyr side chain. The Asp-56(H)/Arg-58(H) salt bridge facilitates access of the P10-Tyr side chain into the binding pocket sculpted by CDRH2 and CDRH3.

CDRH3 contacts the AD-2S1 peptide primarily through a network of backbone H-bonds (Figure 4C). At the apex of the CDRH3 loop, there is a disulphide bond (Supplementary Figure 3) that the peptide appears to 'wrap' around. CDRH3 is encoded by DNA sequences generated by somatic rearrangement and, in part probably, by *de novo* synthesis by TdT. Despite the use of different IGHD genes and N-nucleotides, nine anti-AD-2S1 antibodies exhibited a similar SGLL/I motif in CDRH3, suggesting that these residues were important for binding. The structure of the 8F9–AD-2S1 complex explains why (Figure 4D). The hydroxyl moiety of Ser-100E(H) forms a hydrogen bond with Asp-95(H) to bridge the base of the CDRH3 loop. In the case of the second residue, Gly-100F(H), its lack of a side chain is critical. Any other residue at this position would sterically hinder the important Trp-94(L) residue that forms the base of the pocket for the P8-Leu side chain. The third residue, Leu-100G(H), forms part of the nonpolar surface that contacts P4-Tyr. Finally, Leu-100H(H) makes van der Waals contacts with the Val-96(L) that supports Trp-94(L) that contacts P8-Leu. The IGHD gene-encoded Tyr-100D residue that precedes the SGLL/I motif forms the base of the P10-Tyr-binding pocket (Figure 4E). It is perpendicularly sandwiched between the side chains of Trp-94(L) and P10-Tyr. Tyr-100D(H) also forms a nonpolar contact with the carbonyl group of P8-Leu. There is a Tyr at this position in ITC88 and 2B4, and in all other known anti-AD-2S1 antibodies with one exception, KE5 (McLean *et al*, 2005), where it has been mutated to a conserved Phe. The IGHD-encoded residues N-terminal to the YSGLL/I sequence vary in all three families of anti-AD-2S1 antibodies, which use three different IGHD genes. The structure of the complex of 8F9 Fab and AD-2S1 explains the lack of strict requirements for particular amino-acid residues at these positions. Thus, the interactions between the peptide and CDRH3 are primarily sequence-independent, backbone–backbone interactions. Additionally, residues at the top of the CDRH3 loop make no direct contacts with AD-2S1. Finally, the carbonyl group of Lys-97(H), encoded by bases added by TdT, contacts the backbone nitrogen of P4-Tyr.

Conservation of the structures of 8F9, M2J5 and M2J1

Superimposition of the structures of the unbound 8F9, M2J5 and M2J1 Fab fragments shows that, despite variations in their sequences and large differences in their affinity for
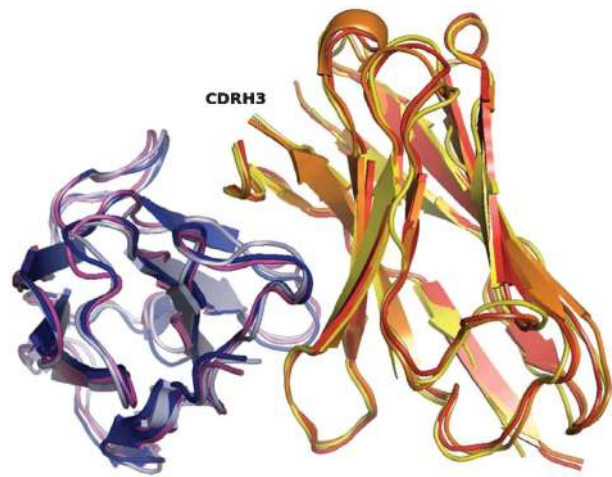

Figure 5 Superimposition of unliganded 8F9, M2J1 and M2J5 Fab fragments. L-chains are shown in purple, blue and light blue for 8F9, M2J5 and M2J1 Fab, respectively. H-chains are shown in red, orange and yellow for 8F9, M2J5 and M2J1, respectively. Note the concordance of the structures and the label pointing out the absence of CDRH3 in each structure.

antigen, there is considerable conservation in the backbone structure of CDRL1, CDRL2 and CDRL3 and CDRH1 (Figure 5). In CDRH2 of M2J1 and M2J5, the electron density for the germline Tyr-58(H) is discontinuous and the B-factors are high (~ 70 Å). Its mutation in 8F9 to Arg likely conferred stability to the loop due a reduction in entropy. CDRH3 was disordered in all three structures of unliganded Fab fragments (Figure 5). The structure of the complex of 8F9 Fab and AD-2S1 showed that, as predicted by the thermodynamic analyses, CDRH3 became ordered upon binding to AD-2S1, although some disorder remained at its apex, where there is no direct contact with the AD-2S1 peptide. Thus, the overall conformations of the CDRs of both chains were conserved following affinity maturation. CDRH3 remained flexible after affinity maturation, although it was stabilized by binding to AD-2S1.

Entropic forces drive affinity maturation

Decreased binding at higher temperatures has been described in unmutated germline-based, polyreactive antibodies, where it is thought to reflect the increased conformational diversity or flexibility of binding sites that enables them to bind a diversity of antigens (Manivel *et al*, 2000; Notkins, 2004; Oppezzo *et al*, 2004). If an antibody undergoes a conformational change when binding an antigen, there is an entropic cost due to the reduction in the conformational degrees of freedom of the CDRs. Typically, this inverse temperature dependence of binding disappears with affinity maturation, coinciding with a more rigid structure of the antibody and a 'lock and key' binding to the antigen (Manivel *et al*, 2000). We observed, however, that even with the hypermutated, affinity-matured 8F9 Fab, its binding to AD-2S1 is inversely correlated with temperature, whether measured by ELISA or Biacore kinetic analyses (Supplementary Figures 4 and 5). To investigate whether 8F9 and M2J5 undergo conformational changes when binding to AD-2S1, we used ITC to analyse the thermodynamic parameters of binding at different temperatures. The results are summarized in Figure 6 and Table I. Throughout the temperature range, ΔG ($\Delta G = \Delta H - T\Delta S$) for
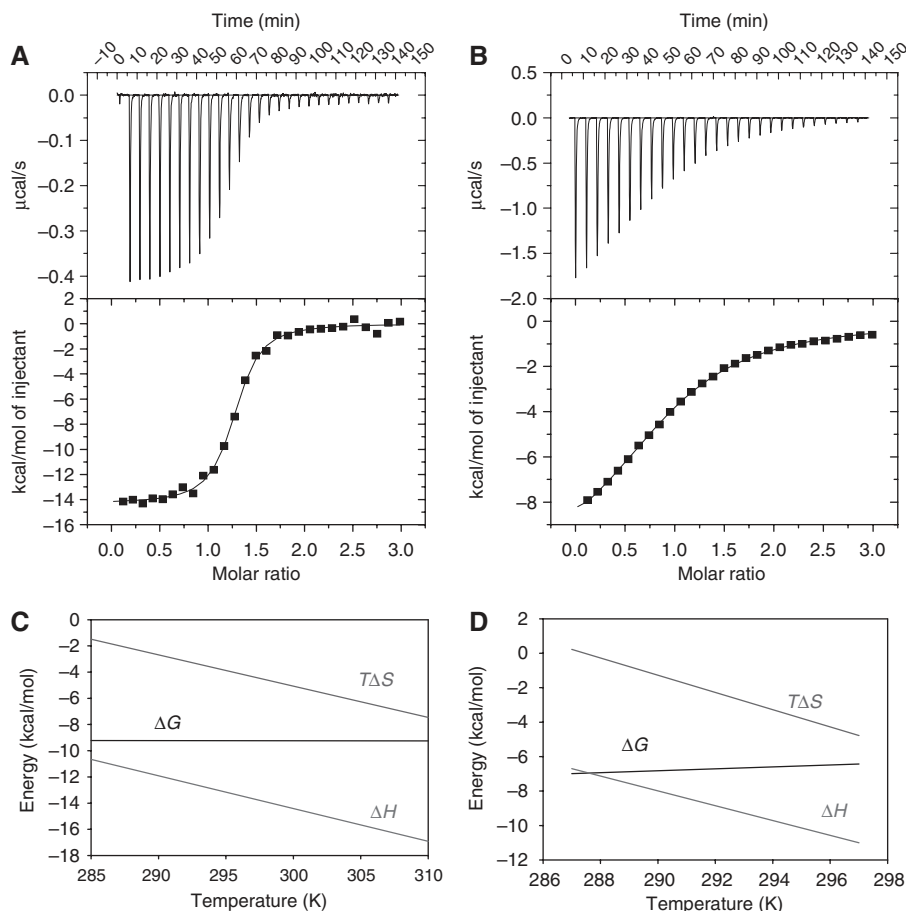
Figure 6 Thermodynamic analysis of AD-2S1 binding to the 8F9 versus M2J5 Fab. Isothermal titration calorimetry of binding to AD-2S1 at 24°C of (**A**) 8F9 Fab and (**B**) M2J5 Fab. The upper plots show the raw titration data with the heat response resulting from each 10 μl injection of AD-2S1 into the ITC cell containing 8F9 Fab or M2J5 Fab. The integrated heats, normalized to the moles of AD-2S1 added and corrected for the heat of dilution (squares), and the nonlinear least-squares fit (line) to a bimolecular interaction are shown below. Thermodynamic parameters from Table I are plotted for 8F9 Fab (**C**) and M2J5 Fab (**D**) binding to AD-2S1 with varying temperature.

the 8F9 Fab remained fairly constant, and, although the entropic penalty increased with increasing temperature, this was compensated for by a favourable increase in enthalpy. The M2J5 Fab exhibited a similar increase in entropic costs of binding at higher temperatures, which was again compensated for with increases in enthalpy. However, the unfavourable entropic change upon binding of the 8F9 Fab to AD-2S1 could result from factors other than a decrease in conformational flexibility of the CDR upon binding. Thus, the entropy of association (ΔS°_{assoc}) is influenced not only by conformational change (ΔS°_{other}) but also by entropic changes resulting from the hydrophobic effect (ΔS°_{HE}) and by a reduction in the rotational and translational degrees of freedom (ΔS°_{rt}). Moreover, we observed that the enthalpic (ΔH) and entropic ($T\Delta S$) contributions to the binding energy (ΔG) varied in a parallel with temperature (Figure 6B). This indicates that a change in heat capacity (ΔC°_{assoc}) was having an important role in the thermodynamics of the association (Spolar and Record, 1994).

ΔC°_{assoc} can be calculated from a plot of ΔH versus temperature. ΔC°_{assoc} of the 8F9 and M2J5 Fab fragments binding to AD-2S1 were found to be −250 and −448 cal/mol K, respectively (Supplementary Table 1). Typically, ΔC°_{assoc} for protein–peptide interactions vary in value from −100 to −1200 cal/mol K (Stites, 1997). The observed values

of −250 and −448 cal/mol K suggest that hydration and the hydrophobic effect have a prominent function in the binding of AD-2S1 by our antibodies.

Spolar and Record (1994) used thermodynamic data to differentiate between 'rigid body' associations and those in which a conformational change takes place with complex formation. In that study, to calculate the contribution of the hydrophobic effect (ΔS°_{HE}) to the entropy of the association, the following equation was utilized:

$$\Delta S^\circ_{HE} = 1.35 \Delta C^\circ_p \ln(T/386)$$

Because there exists a temperature (T_s) where ΔS°_{assoc} is zero;

$$\Delta S^\circ_{assoc} = 0 = \Delta S^\circ_{HE} + \Delta S^\circ_{rt} + \Delta S^\circ_{other}$$

ΔS°_{rt} for protein–protein interactions is ≈ -50 cal/mol K, allowing for the calculation of ΔS°_{other}. Using this equation, calculated values of ΔS°_{other} for 8F9 and M2J5 binding to AD-2S1 were −60 and −128 cal/mol K, respectively (Supplementary Table 1). In comparison, ΔS°_{other} for rigid body associations is zero (Spolar and Record, 1994). Thus, these substantial values of ΔS°_{other} for binding to AD-2S1 suggest that recognition of this viral epitope by both the germline and somatically mutated antibodies is the result of local folding. The fact that the somatically mutated antibody

fragment, 8F9, exhibits half the value of $\Delta S°_{other}$ of M2J5, a germline-based antibody recognizing the same epitope, lends itself to the conclusion that affinity maturation resulted in increased complementarity of the binding site with that of the antigen. However, in contrast to data that suggest that hypermutation of primary immunoglobulins to high-affinity antibodies results in increases in their rigidity and 'lock and key' binding to their target (Wedemayer *et al*, 1997), our data indicate that the high-affinity binding site of 8F9, similar to that of other somatically mutated antibodies (Manivel *et al*, 2000; James *et al*, 2003; Schuermann *et al*, 2005), still exhibits considerable flexibility, which is reduced, but not abolished, by interaction with antigen.

Binding of AD-2S1 to 8F9 results in the addition of three water molecules behind CDRH3 (Figure 4C). This structural evidence of stabilization of CDRH3 upon peptide binding is consistent with the significant $\Delta S°_{other}$ we observed, which indicates that binding involves conformational changes. We also observed eight other water molecules that are present in the binding site of 8F9 in the absence of antigen but are lost when the peptide is bound to 8F9. The loss of these water molecules from hydrophobic surfaces in the antigen-binding site upon antigen binding is consistent with the observed contribution of $\Delta C°_{assoc}$ and $\Delta S°_{HE}$ in the binding of the 8F9 Fab to AD-2S1.

Temperature dependence of binding to a gB fragment

Although all of the above kinetic and thermodynamic analyses have been made with the AD-2S1 peptide, 8F9 and its ancestor M2J1 were presumably selected *in vivo* by the native gB protein. Indeed, M2J1 binds better to a fragment of gB than it does to the AD-2S1 peptide, and the primary ancestor of another family of anti-AD-2S1 antibodies binds only to gB (McLean *et al*, 2005, 2006). Circular dichroism analysis indicates that the secondary structure of the AD-2S1 peptide in solution corresponds to a random coil (data not shown). To examine whether the binding of the 8F9 Fab still varied with temperature when the peptide was conformationally constrained in a folded protein, we expressed an N-terminal fragment of gB (gBNT) that included the AD-2S1 epitope on the surface of mammalian cells (McLean *et al*, 2005). We allowed the 8F9 Fab to associate with the gBNT, washed off unbound Fab, agitated the cells in 10 ml of buffer at different temperatures, and monitored the rate of dissociation of the 8F9 Fab using flow cytometry. The 8F9 Fab dissociated from gBNT at a much lower rate than from the AD-2S1 peptide (Figure 7 and Supplementary Figure 5). This is consistent with the observation that the dissociation of the closely related human anti-AD-2S1 antibody, ITC88, was likewise slower from gB than from the AD-2S1 peptide (Lantto *et al*, 2002). These data suggest that human anti-AD-2S1 antibodies encoded by these V-genes make additional contacts with other residues in gB, and/or that, within the gB protein, the AD-2S1 epitope is constrained in a manner that stabilizes the complex. However, despite this tighter binding of 8F9 Fab to gBNT, there was still a dramatic increase in the rate of dissociation of 8F9 Fab with increasing temperature (Figure 7B). This agrees with structural data that show that, although affinity maturation reduced the conformational flexibility of 8F9, it did not abolish it, and in the absence of ligand, CDRH3 still remained unstructured (Figure 5). It is possible that this flexibility of CDRH3 of 8F9 may have been
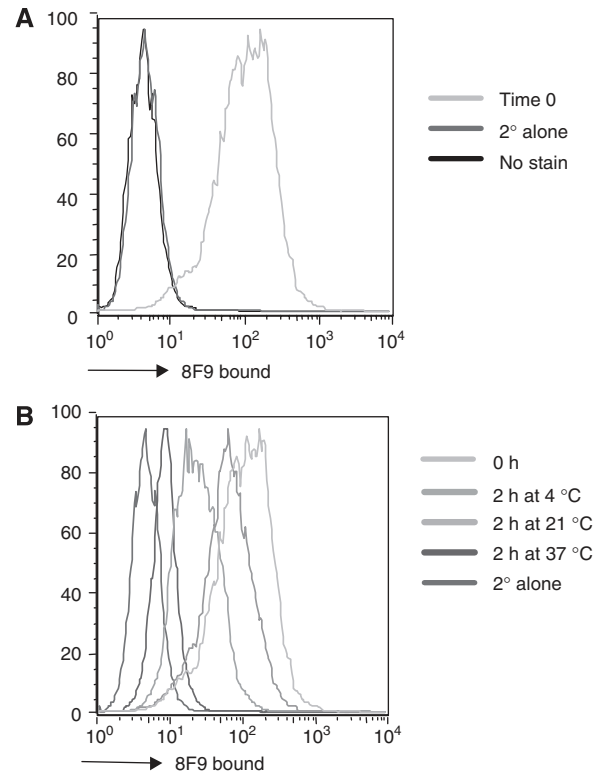
Figure 7 Dissociation of 8F9 Fab from cells expressing the N-terminal amino acids (residues 28–100) of gB. (**A**) Binding of the 8F9 Fab determined by flow cytometry, with comparisons to un-stained cells and cells stained with a secondary anti-human kappa antibody alone. (**B**) Binding of the 8F9 Fab to the N-terminal fragment of gB at time zero and after 2 h of dissociation at 4, 14, 25 and 37°C.

retained during affinity maturation because it was necessary for binding to the AD-2S1 epitope in the native gB protein. Future examination of other antibodies of this family in terms of the flexibility of CDRH3 will be of interest in this regard.

Discussion

Despite extensive somatic mutation of 8F9, germline-encoded residues make all the crucial side chain contacts with the AD-2S1 epitope in the binding site of this high-affinity, somatically mutated neutralizing antibody. The AD2-S1 peptide is contacted by two residues in CDRH3 (Tyr-100D(H), Leu-100G(H)), and seven V-gene-encoded amino-acid side chains. Of these seven V-gene-encoded residues, six remained germline (Tyr-32(L), Arg-91(L), Trp-94(L), Pro95 (L), Asp-53(H), Lys-97(H)), and the other, (Phe-49(L)), although somatically mutated, represented a conservative substitution that preserved the same interactions as the germline residue (Tyr-49(L)). Thus, given that Tyr-100D(H) is encoded by the IGHD gene and that Leu-100G(H) is likely to have been present in the primary immunoglobulin (McLean *et al*, 2005), the somatic mutations that were selected during affinity maturation of M2J1 to 8F9 did not create any new direct contacts between side chains of the antibody and the antigen. The same is likely also the case for ITC88, where, after affinity maturation, all of the seven V-gene-encoded contact residues remained germline, and Tyr-100D(H) and Leu-100G(H) were also conserved. The fact that germline-

encoded contacts with antigen shaped the binding sites of high-affinity, hypermutated antibodies is explained by the physicochemical characteristics of affinity maturation. Thus, analysis of high-resolution structures of complexes of affinity-matured antibodies and antigen indicated that somatic hypermutation generated multiple new antigen contacts in only a minority of combining sites (Ramirez-Benitez and Almagro, 2001). Instead, as in this case, affinity is often improved through enhanced shape complementarity by mutation of non-contact residues in the periphery of the binding site (Tomlinson *et al*, 1996; Li *et al*, 2003). This property of affinity maturation means that germline V-gene-encoded contacts can dictate the architecture of binding sites of high-affinity, protective antibodies.

These data raise the question of whether one of the selective pressures that has shaped the evolution of these V-genes and conserved these contact residues for AD-2S1 was exerted by HCMV. For pathogen-driven selection of V-genes to operate, the pathogen must have been a threat to reproductive success, the V-genes must encode key features of the binding site for a critical target on the pathogen and the target of the protective antibodies must not be readily mutated by the pathogen, presumably because of structural constraints on its function. These criteria are filled in the case of AD-2S1. HCMV has co-evolved with humans, antibodies that target AD-2S1 are neutralizing and will favour reproductive success by limiting infections and by protecting the fetus, and the AD-2S1 epitope varies relatively little across strains of HCMV, perhaps reflecting its functional importance in infectivity (Ohizumi *et al*, 1992). It cannot be proven that evolutionary pressure from HCMV contributed to the conservation of these V-genes. However, the present findings demonstrate unequivocally that human germline V-genes encode key structural features of protective antibodies to a vulnerable and relatively invariant site on an important pathogen and there is likely to be selective pressure against loss of these features.

The evolution of V-genes that encode key contacts with vulnerable sites on pathogens could be termed 'innate immunological memory'. Its unique feature, not provided by acquired, somatic immunological memory, is the capacity to selectively target vulnerable sites on the pathogen. Only innate mechanisms, honed by evolutionary pressure from past battles with a pathogen, can provide a historical 'memory' of where antibodies should be aimed to protect against that pathogen. A pathogen will only drive the selection of those V-genes that protect against that pathogen. In contrast, although somatically acquired immunological memory delivers high-affinity antibodies, it is blind to whether those antibodies are protective, irrelevant or even harmful.

There is evidence for V-gene-encoded innate immunological memory in the antibody response against other pathogens that have co-evolved with humans and that exhibit relatively invariable targets for protective antibodies. These include the capsular polysaccharides of *Haemophilus influenzae* (Insel *et al*, 1992; Lucas *et al*, 1998; Hougs *et al*, 1999; Lucas and Reason, 1999) or *Streptococcus pneumoniae* (Lucas *et al*, 1998; Sun *et al*, 1999; Zhou *et al*, 2002), which are targets for protective antibodies that promote phagocytosis (Bruyn *et al*, 1992). Indeed, in the case of one subtype of *S. pneumoniae*, 23F, antibodies against the 23F pneumococcal polysaccharide frequently use exactly the

same pair of V-genes used in AD-2S1 antibodies, although significantly there are differences in CDRH3 and CDRL3 (Zhou *et al*, 2002).

This 'multi-tasking' is consistent with evidence that a single pair of V-genes recombined with different CDRH3 can give rise to high-affinity antibodies against multiple antigens (Davis, 2004). Indeed, M2J1 itself is polyspecific and recognizes multiple autoantigens, although it nevertheless exhibited fine sequence specificity for AD-2S1 in that it failed to bind detectably to the homologous peptide from CCMV (McLean *et al*, 2006). The polyspecificity of primary immunoglobulins may depend on the degree of conformational flexibility of CDR loops (Manivel *et al*, 2000; James *et al*, 2003), different orientation of antigens within the same binding site (Sethi *et al*, 2006) or conformational isomerism (James *et al*, 2003). *IGHV3-30* and *IGKV3-11* are clearly versatile and are frequently paired with different V-genes in human antibodies against a wide variety of antigens. The versatility of binding sites of primary immunoglobulins may be important for pathogen-driven selection of V-genes, enabling V-genes to be selected to encode contact residues for targets on pathogens without unduly restricting the repertoire for novel antigens and enabling single V-genes to 'multi-task' in encoding structural features of protective antibodies against multiple pathogens. Multi-tasking is a common feature of innately encoded immune receptors: for example, both TLR-4 and CD14 recognize not only lipopolysaccharide but also the fusion protein of respiratory syncytial virus and many other ligands (Finberg *et al*, 2004). V-genes are likely to have been subject to two complimentary selective pressures to encode both conformational versatility and contact residues that sculpt the binding sites for vulnerable sites on pathogens.

Materials and methods

Peptide synthesis
For kinetic and thermodynamic experiments, the peptide (SHRA-N**ETIYNTTLKY**) containing the AD-2S1 epitope of HCMV gB was synthesized with and without a biotin group added to the N terminus by solid-phase synthesis (Phil Owen, The Biomedical Research Centre, Vancouver, Canada). For use in X-ray crystallography experiments, a shorter peptide composed of the minimal epitope, in bold above, was synthesized.

Fab purification
cDNA encoding the H- and L-chains of each Fab were cloned separately into pET vectors so that there was a $6 \times$ His tag present on the C terminus of the H-chain. The vectors were expressed in *E. coli* and, after induction with IPTG, cells were harvested and lysed in 50 mM Tris, 50 mM Tris, 2 mM EDTA, 0.5% Triton X-100 with the addition of Complete Mini Protease Inhibitor Tablets (Roche). Inclusion bodies were isolated by centrifugation and resuspended in solubilization buffer (50 mM Tris, pH 8, 6 M GuHCl, 10 mM DTT). The solubilized material was diluted 50% in 50 mM Tris, pH 8, 2 M GuHCl and dialysed overnight against this buffer at 4°C. The dialysis buffer was then changed to 50 mM Tris, pH 8, 1 M GuHCl, 0.4 M arginine, 3 mM reduced glutathione and 0.9 mM oxidized glutathione. The following day, the dialysis buffer was changed by reducing the GuHCl concentration to 0.5 M and the following day, the buffer was changed to one with no GuHCl. Following this refolding procedure, residual unfolded protein was removed by centrifugation and the soluble Fab was purified sequentially with a combination of His-affinity chromatography and cationic exchange FPLC. Refolding of the Fabs was verified by circular dichroism analysis.

X-ray crystallography

The 8F9 Fab was dissolved in 20 mM Tris–HCl, pH 8.0 at 8 mg/ml with 1 mM AD-2S1 peptide dissolved in buffer. For crystallization, we used the hanging drop method at room temperature. For crystallizing the complex of the 8F9 Fab and the AD-2S1 peptide, the well solution contained 1.9 M ammonium sulphate with 0.10 M CAPS buffer, pH 10.6. 8F9 Fab was crystallized in the absence of peptide using the same conditions but with the addition of 5% dioxane in the well solution. M2J1 and M2J5 Fabs were similarly crystallized using 2.6 M ammonium sulphate and 2% PEG 400 in the well solution. Crystals were soaked in well solution containing increasing concentrations of glycerol from 1 to 25% and cooled to 110°K prior to data collection. Data for the complex of the 8F9 Fab and peptide, and for the M2J5 Fab were collected on a Rigaku RU-300 copper anode home source X-ray machine. Data for the 8F9 Fab without the peptide, and for the M2J1 Fab were collected at the APS synchrotron using beamlines BM19 and BM14C, respectively. The structure of the complex of the 8F9 Fab and the peptide was determined by molecular replacement using PDB ID 1HEZ with the CDR loops removed and the elbow angle shifted $+2°$. All other structures were determined by molecular replacement using the 8F9 Fab model. Modelling and refinements were carried out using CNS (Brunger *et al*, 1998) and Coot (Emsley and Cowtan, 2004). All structure figures were generated using the Pymol Molecular Graphics System (Delano Scientific). Data collection and structure refinement statistics are found in Supplementary Table 2. Representative electron density maps for each structure are found in Supplementary Figure 6.

ELISA

The 15-mer AD-2S1 peptide with biotin (2 μg/ml) was incubated in streptavidin-coated 96-well plates (Nunc) for 2 h at room temperature. Wash buffer (PBS + 0.05% Tween-20) was used to remove unbound peptide quickly using a SkanWasher 300 (Skatron). Serially diluted Fabs were added to the wells for either 1 h at 37°C (Supplementary Figure 1) or for 2 h at 4, 25 or 37°C (Supplementary Figure 4). Unbound Fabs were decanted and the plates were washed as above. Alkaline phosphatase-coupled goat anti-human kappa secondary antibodies were added for 1 h at 37°C before washing and the addition of substrate for quantification.

SPR analysis

Kinetic analysis of the 8F9 Fab binding to the AD-2S1 containing peptide was performed on a Biacore 3000 (Biacore AB Inc., Uppsala, Sweden). The AD-2S1 peptide containing an N-terminal biotin was immobilized on a streptavidin-coated chip (cat. no. BR-1003-98) at a low surface density (13 RU) to allow for accurate kinetic determinations. At this density, initial binding rates were independent of flow rate and a mass transfer influence was ruled out. 8F9 Fab binding to AD-2S1 was monitored at a flow rate of 20 μl/min in HBS containing 0.01% surfactant p-20 and at concentrations ranging from 3 to 100 nM. An injection of buffer alone was included and the multichannel injection mode utilized so as to include an in-line reference cell to account for changes in the bulk refractive index. The 8F9 Fab association rate constant (k_a), dissociation rate constant (k_d) and affinity constant (K_D) were calculated using BIAevaluation 4.1 software (Biacore AB). Curves were fitted using a 1:1 (Langmuir) binding model.

ITC

For ITC experiments, Fabs were dialysed to 10 mM HEPES, pH 7.8, 150 mM NaCl, with peptide being diluted in the same buffer. All ITC experiments were performed in a MicroCal VP-ITC at the temperatures indicated. For experiments with 8F9, the Fab was placed in the calorimeter cell (volume = 1.4242 ml) at a concentration of 6.4 μM and a solution of AD-2S1 (91 μM) was titrated into the cell with 10 μl injections using a rotating stirrer syringe. For experiments with M2J5, the M2J5 Fab was at 57 μM and a more concentrated solution of AD-2S1 (810 μM) was injected. Binding stoichiometry (n), enthalpy (ΔH) and equilibrium association constants (K_a) were determined by fitting the data, corrected for the heat of dilution of the titrant AD-2S1, to a 1:1 biomolecular interaction model using the Origin 7 software supplied by the manufacturer.

Flow cytometry analysis

NSO murine myeloma cells engineered to stably express an N-terminal fragment of gB that contained the AD-2S1 epitope were described previously (McLean *et al*, 2005). Cells were fixed in 4% paraformaldehyde for 10 min on ice, washed in PBS + 5% FBS, and held on ice for 20 min with saturating amounts of the 8F9 Fab. Cells were washed and suspended in 10 ml of PBS + 5% FBS. One aliquot was immediately stained for bound 8F9 Fab by mixing it with FITC-conjugated anti-human kappa antibodies (Southern Biotechnology Associates) for 5 min on ice, after which the cells were washed and the levels of fluorescence were quantified by flow cytometry. The remaining aliquots were held for 2 h at 4, 14, 25 or 37°C after which they were stained with the FITC anti-kappa antibodies and the levels of bound 8F9 Fab remaining were quantified by flow cytometry.

Supplementary data

Supplementary data are available at *The EMBO Journal* Online (http://www.embojournal.org).

Acknowledgements

References

Batista FD, Neuberger MS (1998) Affinity dependence of the B cell response to antigen: a threshold, a ceiling, and the importance of off-rate. *Immunity* **8:** 751–759

Boppana SB, Pass RF, Britt WJ, Stagno S, Alford CA (1992) Symptomatic congenital cytomegalovirus infection: neonatal morbidity and mortality. *Pediatr Infect Dis J* **11:** 93–99

Brunger AT, Adams PD, Clore GM, DeLano WL, Gros P, Grosse-Kunstleve RW, Jiang JS, Kuszewski J, Nilges M, Pannu NS, Read RJ, Rice LM, Simonson T, Warren GL (1998) Crystallography & NMR system: a new software suite for macromolecular structure determination. *Acta Crystallogr D Biol Crystallogr* **54:** 905–921

Bruyn GA, Zegers BJ, van Furth R (1992) Mechanisms of host defense against infection with *Streptococcus pneumoniae*. *Clin Infect Dis* **14:** 251–262

Davis MM (2004) The evolutionary and structural 'logic' of antigen receptor diversity. *Semin Immunol* **16:** 239–243

Desiderio SV, Yancopoulos GD, Paskind M, Thomas E, Boss MA, Landau N, Alt FW, Baltimore D (1984) Insertion of N regions into heavy-chain genes is correlated with expression of terminal deoxytransferase in B cells. *Nature* **311:** 752–755

Duff P (2005) Immunotherapy for congenital cytomegalovirus infection. *N Engl J Med* **353:** 1402–1404

Emsley P, Cowtan K (2004) Coot: model-building tools for molecular graphics. *Acta Crystallogr D Biol Crystallogr* **60:** 2126–2132

Finberg RW, Re F, Popova L, Golenbock DT, Kurt-Jones EA (2004) Cell activation by Toll-like receptors: role of LBP and CD14. *J Endotoxin Res* **10:** 413–418

Hougs L, Juul L, Ditzel HJ, Heilmann C, Svejgaard A, Barington T (1999) The first dose of a *Haemophilus influenzae* type b conjugate vaccine reactivates memory B cells: evidence for extensive clonal selection, intraclonal affinity maturation, and multiple isotype switches to IgA2. *J Immunol* **162:** 224–237

Insel RA, Adderson EE, Carroll WL (1992) The repertoire of human antibody to the *Haemophilus influenzae* type b capsular polysaccharide. *Int Rev Immunol* **9:** 25–43

James LC, Roversi P, Tawfik DS (2003) Antibody multispecificity mediated by conformational diversity. *Science* **299:** 1362–1367

Lang J, Jackson M, Teyton L, Brunmark A, Kane K, Nemazee D (1996) B cells are exquisitely sensitive to central tolerance and receptor editing induced by ultralow affinity, membrane-bound antigen. *J Exp Med* **184:** 1685–1697

Lantto J, Fletcher JM, Ohlin M (2002) A divalent antibody format is required for neutralization of human cytomegalovirus via antigenic domain 2 on glycoprotein B. *J Gen Virol* **83:** 2001–2005

Lefranc MP, Clement O, Kaas Q, Duprat E, Chastellan P, Coelho I, Combres K, Ginestoux C, Giudicelli V, Chaume D, Lefranc G (2005) IMGT-Choreography for immunogenetics and immunoinformatics. *In Silico Biol* **5:** 45–60

Li Y, Li H, Yang F, Smith-Gill SJ, Mariuzza RA (2003) X-ray snapshots of the maturation of an antibody response to a protein antigen. *Nat Struct Biol* **10:** 482–488

Lucas AH, Moulton KD, Reason DC (1998) Role of kappa II-A2 light chain CDR-3 junctional residues in human antibody binding to the *Haemophilus influenzae* type b polysaccharide. *J Immunol* **161:** 3776–3780

Lucas AH, Reason DC (1999) Polysaccharide vaccines as probes of antibody repertoires in man. *Immunol Rev* **171:** 89–104

Makela O, Kaartinen M (1988) Genetic control of early antibody responses. *Immunol Rev* **105:** 85–96

Manivel V, Bayiroglu F, Siddiqui Z, Salunke DM, Rao KV (2002) The primary antibody repertoire represents a linked network of degenerate antigen specificities. *J Immunol* **169:** 888–897

Manivel V, Sahoo NC, Salunke DM, Rao KV (2000) Maturation of an antibody response is governed by modulations in flexibility of the antigen-combining site. *Immunity* **13:** 611–620

McGeoch DJ, Dolan A, Ralph AC (2000) Toward a comprehensive phylogeny for mammalian and avian herpesviruses. *J Virol* **74:** 10401–10406

McLean GR, Cho CW, Schrader JW (2006) Autoreactivity of primary human immunoglobulins ancestral to hypermutated human antibodies that neutralize HCMV. *Mol Immunol* **43:** 2012–2022

McLean GR, Olsen OA, Watt IN, Rathanaswami P, Leslie KB, Babcock JS, Schrader JW (2005) Recognition of human cytomegalovirus by human primary immunoglobulins identifies an innate foundation to an adaptive immune response. *J Immunol* **174:** 4768–4778

Meyer H, Masuho Y, Mach M (1990) The gp116 of the gp58/116 complex of human cytomegalovirus represents the amino-terminal part of the precursor molecule and contains a neutralizing epitope. *J Gen Virol* **71** (Part 10)**:** 2443–2450

Muller S, Wang H, Silverman GJ, Bramlet G, Haigwood N, Kohler H (1993) B-cell abnormalities in AIDS: stable and clonally-restricted antibody response in HIV-1 infection. *Scand J Immunol* **38:** 327–334

Nigro G, Adler SP, La Torre R, Best AM (2005) Passive immunization during pregnancy for congenital cytomegalovirus infection. *N Engl J Med* **353:** 1350–1362

Notkins AL (2004) Polyreactivity of antibody molecules. *Trends Immunol* **25:** 174–179

Ohizumi Y, Suzuki H, Matsumoto Y, Masuho Y, Numazaki Y (1992) Neutralizing mechanisms of two human monoclonal antibodies against human cytomegalovirus glycoprotein 130/55. *J Gen Virol* **73** (Part 10)**:** 2705–2707

Ohlin M, Sundqvist VA, Mach M, Wahren B, Borrebaeck CA (1993) Fine specificity of the human immune response to the major neutralization epitopes expressed on cytomegalovirus gp58/116 (gB), as determined with human monoclonal antibodies. *J Virol* **67:** 703–710

Oppezzo P, Dumas G, Bouvet JP, Robello C, Cayota A, Pizarro JC, Dighiero G, Pritsch O (2004) Somatic mutations can lead to a loss of superantigenic and polyreactive binding. *Eur J Immunol* **34:** 1423–1432

Qi H, Egen JG, Huang AY, Germain RN (2006) Extrafollicular activation of lymph node B cells by antigen-bearing dendritic cells. *Science* **312:** 1672–1676

Ramirez-Benitez MC, Almagro JC (2001) Analysis of antibodies of known structure suggests a lack of correspondence between the residues in contact with the antigen and those modified by somatic hypermutation. *Proteins* **45:** 199–206

Schuermann JP, Prewitt SP, Davies C, Deutscher SL, Tanner JJ (2005) Evidence for structural plasticity of heavy chain complementarity-determining region 3 in antibody-ssDNA recognition. *J Mol Biol* **347:** 965–978

Sethi DK, Agarwal A, Manivel V, Rao KV, Salunke DM (2006) Differential epitope positioning within the germline antibody paratope enhances promiscuity in the primary immune response. *Immunity* **24:** 429–438

Spolar RS, Record Jr MT (1994) Coupling of local folding to site-specific binding of proteins to DNA. *Science* **263:** 777–784

Stites WE (1997) Proteinminus signprotein interactions: interface structure, binding thermodynamics, and mutational analysis. *Chem Rev* **97:** 1233–1250

Sun Y, Park MK, Kim J, Diamond B, Solomon A, Nahm MH (1999) Repertoire of human antibodies against the polysaccharide capsule of *Streptococcus pneumoniae* serotype 6B. *Infect Immun* **67:** 1172–1179

Tanaka T, Nei M (1989) Positive Darwinian selection observed at the variable-region genes of immunoglobulins. *Mol Biol Evol* **6:** 447–459

Thai TH, Purugganan MM, Roth DB, Kearney JF (2002) Distinct and opposite diversifying activities of terminal transferase splice variants. *Nat Immunol* **3:** 457–462

Tomlinson IM, Walter G, Jones PT, Dear PH, Sonnhammer EL, Winter G (1996) The imprint of somatic hypermutation on the repertoire of human germline V genes. *J Mol Biol* **256:** 813–817

Wedemayer GJ, Patten PA, Wang LH, Schultz PG, Stevens RC (1997) Structural insights into the evolution of an antibody combining site. *Science* **276:** 1665–1669

Zhou J, Lottenbach KR, Barenkamp SJ, Lucas AH, Reason DC (2002) Recurrent variable region gene usage and somatic mutation in the human antibody response to the capsular polysaccharide of *Streptococcus pneumoniae* type 23F. *Infect Immun* **70:** 4083–4091